A RESTORATION METHOD FOR CONFOCAL MICROSCOPY USING COMPLEX WAVELET TRANSFORM

G. Pons Bernad, L. Blanc-Féraud and J. Zerubia

Ariana Research Group, INRIA/I3S, 2004 route des Lucioles - BP93, 06902 Sophia Antipolis, France

email: Firstname.Lastname@sophia.inria.fr

ABSTRACT

Confocal laser scanning microscopy is a powerful and increasingly popular technique for 3D imaging of biological specimens. However the acquired images are degraded by blur from out-of-focus light and Poisson noise due to photon-limited detection. Several deconvolution and/or denoising methods have been proposed to reduce these degradations.

Here we propose a wavelet denoising method, which turns out to be very effective for three-dimensional confocal images. To obtain a translation and rotation invariant algorithm, we have developped the 3D Complex Wavelet Transform introduced by N. Kingsbury. These wavelets allow moreover a better directional selectivity of the wavelet coefficients. We show on simulated and real biological data the good performances of this algorithm.

1. INTRODUCTION

The confocal laser scanning microscope (CLSM) is an optical fluorescence microscope associated to a laser that scans the specimen in 3D and uses a pinhole to reject most out-of-focus light. The quality of confocal microscopy images suffers from two basic physical limitations. First, out-of-focus blur due to the diffraction-limited nature of optical microscopy remains substantial, even though it is reduced compared to widefield microscopy. Second, the confocal pinhole drastically reduces the amount of light detected by the photomultiplier, leading to Poisson noise. The images produced by CLSM can therefore benefit from postprocessing by deconvolution methods designed to reduce blur and/or noise. Image deconvolution methods can be classified into two families, whether they are multiresolution or not. In confocal microscopy, non multiresolution methods include the iterative methods such as Tikhonov-Miller inverse filter [1], the Carrington [1], Richardson-Lucy (RL) algorithms [2, 3], Conchello et al. [4], van Kempen et al. [5] and Dey et al. [6]. On the other hand, the multiresolution methods consist of representing an image at various levels of resolution, and restoring separately the different scales. Boutet de Monvel et al. [7] have proposed a real wavelet basis for denoising and a non-regularized Richardson-Lucy method for deconvolution. In [8], Willett et al. use a multiscale approach based on platelets to denoise 2D images in the presence of a Poisson noise. Here we concentrate on denoising algorithms and we will demonstrate that the 3D Complex Wavelet Transform (CWT) is well adapted to the confocal biological imagery.

We first propose a denoising algorithm based on complex wavelet thresholding by using the 3D CWT which provides invariance and directional properties. We present experimental results on synthetic data (section 3.1), showing that CWT results outperform results using standard real wavelet transform. We then show experimental results on real data (section 3.2). Finally, we conclude in section 4 and give some perspectives for future research work.

2. THE DENOISING ALGORITHM

2.1. 3D Complex Wavelet Transform

N. Kingsbury [9] introduced the Complex Wavelet Transform (CWT) a few years ago. Here we have developed a 3-D CWT, following the original work of N. Kingsbury in 2D and 3D. In the transform defined by N. Kingsbury, the first level of a real biorthogonal transform is undecimated, defining a perfect invariance at level 1. The coefficients are re-ordered into 8 interleaved images by using their parity. This defines the 8 trees $T = A, B, C, D, E, F, G, H$ which are redundant. For $j > 1$, each tree is processed separately with a combination of odd, h^o and g^o, and even, h^e and g^e, filters depending on each tree. The subbands are indexed by k. Finally, the detail subbands $d^{j\,k}$ of the parallel trees are combined to form 4 complex subbands.

Thresholding the magnitudes $|z_{\pm}|$ without modifying the phase enables to define a nearly shift invariant filtering method.

The details of the 7 subbands hgh, ghh, hhg, ggh, hgg, ghg and ggg give 28 complex subbands, instead of 7 in the real case. This directional separation is made possible by using filters that have an asymmetric response. Thus, negative and positive frequencies can be separed which provides a strong orientation of the impulse responses and therefore a high directional selectivity between the different subbands.

2.2. The proposed algorithm

We deal with the case of denoising non-blurred confocal images contaminated by a Poison distribution. Here we suppose that the number of detected photons are important enough to be approximated by a Gaussian noise. The degradation model is represented by the equation:

$$Y = X + n \tag{1}$$

where Y is the observed data, X is the original image and n is the additive white Gaussian noise with standard deviation σ.

Authors like e.g. Donoho et al. [10], Kalifa and Mallat [11], have proposed to denoise the image using a real wavelet basis. This is achieved by cancelling the coefficients below a given threshold. We have employed the three thresholding functions (soft, hard and Oracle) defined in [10], using a threshold $T_k = 1.6\sigma_k$ as proposed by Kalifa in [11]. However, the real wavelet transform is not shift invariant, which produces artefacts. Also, it is not rotation invariant because of its separability. That is why we have applied the CWT to image denoising which is only 2^d redundant where d is the dimension of the space ($d = 3$ in 3D applications).

The proposed denoising algorithm consists of the following steps:

- Complex Wavelet Transform (3D-CWT) of Y
- Conversion from octet-tree to complex transform
- Estimation of σ_k, numerically computed from σ (known for synthetic images and manually estimated, from different homogeneous areas, for real biological images)
- Soft-thresholding of noisy coefficients y for each subband k
- Conversion from complex transform to octet-tree
- Inverse CWT, which gives the estimate $\hat{X}$.

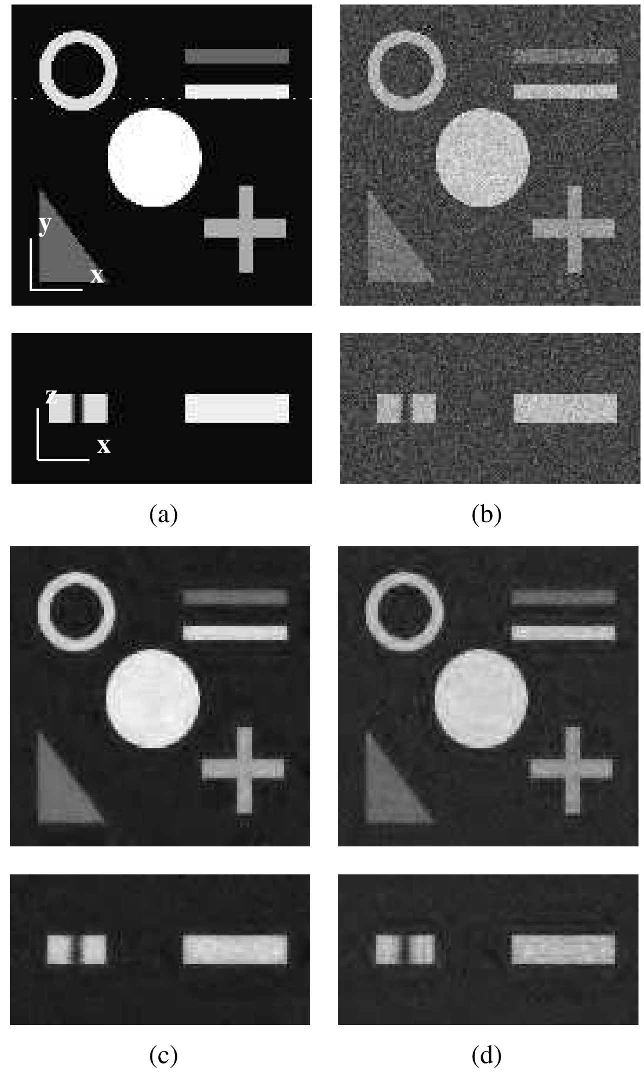

Fig. 1. Denoising of synthetic $128x128x64$ test image with 1 pixel for 250nm in XY, and 1 pixel for 600nm for XZ. One cut of the 3D image is shown. First row: (a) original and (b) noisy image; second row: (c) image denoised by CWT with $\Delta SNR = 15.36$ dB and (d) image denoised by real wavelet with $\Delta SNR = 13.49$ dB.

3. RESULTS

3.1. Results on simulated images

We have compared the proposed denoising method (using the CWT) with the classical wavelet denoising method (using the real wavelet) on 3D simulated data. To quantify the quality of the techniques we have used the difference of Signal to Noise Ratio (ΔSNR) between the SNR of the denoised image and the degraded image.

Fig. 1 (a) represents the original image, (b) the degraded one by a Gaussian noise with variance $\sigma^2 = 900$. We have realized three scales of the wavelet decomposition and used the soft-thresholding function. The degraded image before denoising have a $SNR = 2.87$ dB. The result obtained by the CWT denoised algorithm is shown in (c) with $\Delta SNR = 15.36$ dB and in (d) the denoised image by applying the real wavelet with $\Delta SNR = 13.49$ dB. We observe that image (d) shows more intensity oscillations at the edges of the object. Moreover, we can notice that image (c) better preserves the borders.

Fig. 2 (a) represents a textured image with a fine structure, (b) the degraded image by a Gaussian noise with variance $\sigma^2 = 900$. We have chosen as previously, three scales of the wavelet decomposition and used the soft- thresholding function. The degraded image before denoising have a $SNR = -1.20$ dB. The result obtained by the CWT denoising algorithm is shown in (c) with $\Delta SNR = 13.12$ dB and in (d) appears the denoised image by applying the real wavelet with $\Delta SNR = 11.45$ dB.

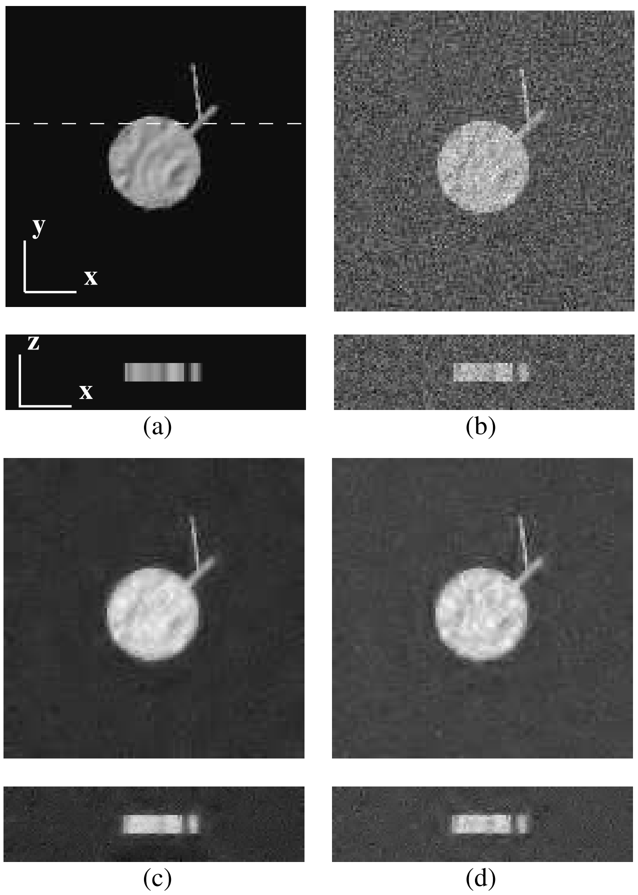

Fig. 2. Denoising of synthetic 128x128x32 test image with 1 pixel for 250nm in XY, and 1 pixel for 600nm for XZ. One cut of the 3D image is shown. First row: (a) original and (b) noisy image; second row: (c) image denoised by CWT with $\Delta SNR = 14.32$ dB and (d) image denoised by real wavelet transform with $\Delta SNR = 12.65$ dB.

Fig. 3 shows the results of a set of denoising experiments performed on the test image (see Fig. 1 (a)) degraded by various levels of noise. For each level of noise, the gain in SNR was measured.

In conclusion, complex wavelet denoising leads qualitatively to better results than real wavelet denoising.

We remark that, for each thresholding function, the CWT always overcomes the real wavelet transform from 2 dB. In all our tests the soft-thresholding function gives the best results, followed by the Oracle thresholding, then by the hard-thresholding.

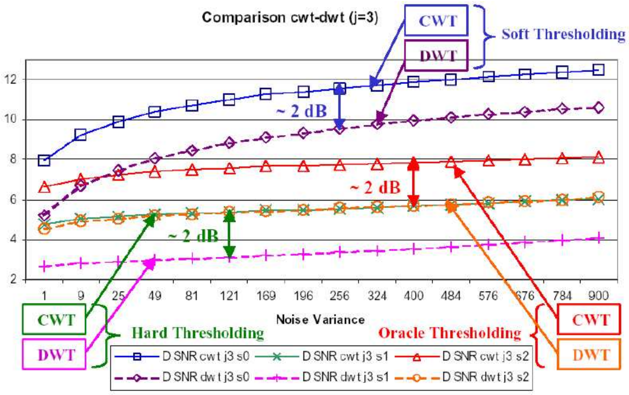

Fig. 3. Denoising of image Fig. 1 (a) by CWT and real wavelet transform for different thresholding functions (soft, hard and Oracle) and different noise variances.

3.2. Results on real biological data

In this section, we present experimental results of the proposed algorithm. Fig. 4 (a) shows one cut extracted from a 3D image, imaging a Drosophila embryo realizing the dorsal closing. Fig. 4 (b) is the denoised image by the proposed algorithm. We remark that the result is satisfactory, the borders of the structures are well preserved while the noise has been removed.

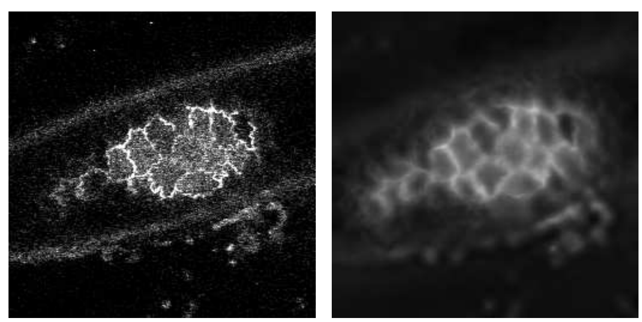

(a) (b)

Fig. 4. A Drosophila embryo realizing the dorsal closing. One view extracted from a 3D image (256x256x30). Acquisition performed with a Zeiss Axiovert 200 with an objective of 40x, NA = 1.3. (a) raw image; (b) denoised image. (© UMR 6543 CNRS/Laboratoire J.-A. Dieudonné).

Fig. 5 presents the results of the proposed denoising algorithm for a cluster of 4 fluorescent beads of 6 μm acquired with a Zeiss Axiovert 200M confocal microscope. Here we observe the good results, too.

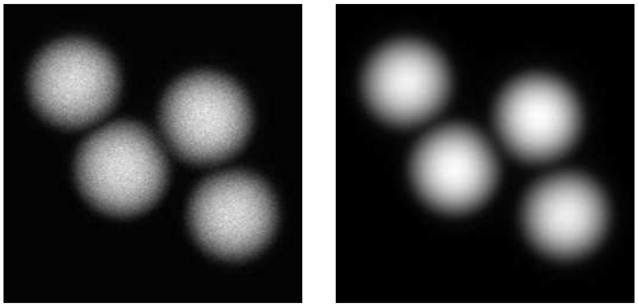

(a) (b)

Fig. 5. A cluster of 4 fluorescent beads of 6 μm. One view extracted from a 3D image. (© Quantative Image Analysis Group, CNRS URA 1947, Institut Pasteur). The stack is 256x256x128 with voxels of size 89x89x230 nm. Acquisition performed with a Zeiss Axiovert 200M confocal microscope, with an internal magnification (given by the manufacturer) of 3.3x. The objective is a 63x/1.4 NA plan Apochromat. (a) raw image; (b) denoised image.

4. CONCLUSION AND PERPECTIVES

In this paper, we have presented a denoising approach for confocal microscopy, based on the complex wavelet transform. Noise is efficiently removed from the images, and the objets are well preserved as shown on synthetic and real biological data.

In a near future, the proposed denoising algorithm will be integrated into a whole package comprising also a deconvolution step. This is the object of our current research and will be presented in another paper.

5. ACKNOWLEDGEMENTS

The authors would like to thank Prof. Nick Kingsbury (from the Signal Processing Group, Dept. of Eng., Cambridge University) and André Jalobeanu (from NASA Ames Research Center, CA, USA) for many intesting discussions. A special thank to J.C. Olivo-Marin, C. Zimmer and P. Roux from Institut Pasteur for providing the image of Fig. 5 and for interesting comments. The image of Fig. 4 has been provided by Fanny Pignolé (UMR 6543 CNRS / J.-A. Dieudonné), Luis Almeida (Laboratoire J.-A. Dieudonné) and Stéphane Noselli (UMR 6543 CNRS).

This work is funded by the DeMiTri cooperative research action (*http://www-sop.inria.fr/ariana/demitri.html*).

6. REFERENCES

[1] G.M.P. van Kempen, L.J. van Vliet, P.J. Verveer, and H.T.M van der Voort, "A quantitative comparison of image restoration methods for confocal microscopy," *J. of Microscopy*, vol. 185, pp. 354–365, Mar. 1997.

[2] W. H. Richardson, "Bayesian-based iterative method of image restoration," *J. of Opt. Soc. of Am.*, vol. 62, pp. 55–59, 1972.

[3] L.B. Lucy, "An iterative technique for rectification of observed distributions," *The Astronomical Journal*, vol. 79, no. 6, pp. 745–765, 1974.

[4] J.-A. Conchello and J.G. McNally, "Fast regularization technique for expectation maximization algorithm for optical sectioning microscopy," *Three-Dimensional and Multidimensional Microscopy: Image Acquisition and Processing III*, pp. 199–208, 1996.

[5] G.M.P. van Kempen and L.J. van Vliet, "Background estimation in non linear image restoration," *Journal of Optical Society of America A*, vol. 17, no. 3, pp. 425–433, Mar. 2000.

[6] N. Dey, L. Blanc-Féraud, C. Zimmer, Z. Kam, J.-C. Olivo-Marin, and J. Zerubia, "A deconvolution method for confocal microscopy with total variation regularization," in *Proceedings of ISBI'2004*, April 2004.

[7] J. Boutet de Monvel, S. Le Calvez, and M. Ulfendahl, "Image Restoration for Confocal Microscopy: Improving the Limits of Deconvolution, with Application to the Visualization of the Mammalian Hearing Organ," *Biophysical Journal*, vol. 80, pp. 2455–2470, May 2001.

[8] R. Willett and R.D. Nowak, "Platelets: a multiscale approach for recovering edges and surfaces in photon-limited medical imaging," *IEEE Trans. on Medical Imaging*, vol. 22, no. 3, pp. 332–350, Mar. 2003.

[9] N. Kingsbury, "The dual-tree complex wavelet transform : a new efficient tool for image restoration and enhancement," *Proc. of EUSIPCO, Thodes, Greece*, pp. 319–322, 1998.

[10] D.L. Donoho and I.M.Johnstone, "Ideal spatial adaptation via wavelet shrinkage," *Biometrika*, vol. 81, pp. 425–455, 1994.

[11] J. Kalifa and S. Mallat, *Bayesian inference in wavelet based methods*, chapter Minimax restoration and deconvolution, Springer, 1999.